HAL
open science

DOUBLE PROBE APPROACH TO PROTEIN ADSORPTION ON POROUS CARBON SURFACES

Balázs Nagy, Ajna Tóth, Irina Savina, Sergey Mikhalovsky, Lyuba Mikhalovska, Erik Geissler, Krisztina Laszlo

To cite this version:

Balázs Nagy, Ajna Tóth, Irina Savina, Sergey Mikhalovsky, Lyuba Mikhalovska, et al.. DOUBLE PROBE APPROACH TO PROTEIN ADSORPTION ON POROUS CARBON SURFACES. Carbon, 2017, 112, pp.103 - 110. 10.1016/j.carbon.2016.10.095 . hal-01657352

HAL Id: hal-01657352

https://hal.science/hal-01657352v1

Submitted on 6 Dec 2017

HAL is a multi-disciplinary open access archive for the deposit and dissemination of scientific research documents, whether they are published or not. The documents may come from teaching and research institutions in France or abroad, or from public or private research centers.

L'archive ouverte pluridisciplinaire **HAL**, est destinée au dépôt et à la diffusion de documents scientifiques de niveau recherche, publiés ou non, émanant des établissements d'enseignement et de recherche français ou étrangers, des laboratoires publics ou privés.

DOUBLE PROBE APPROACH TO PROTEIN ADSORPTION ON POROUS CARBON SURFACES

Balázs Nagy,[a] Ajna Tóth,[a] Irina Savina,[b] Sergey Mikhalovsky,[b] Lyuba Mikhalovska,[b] Erik Geissler,[c] Krisztina László[a,*]

[a]Department of Physical Chemistry and Materials Science, Budapest University of Technology and Economics, H-1521 Budapest, Hungary

[b]School of Pharmacy and Biomolecular Sciences, University of Brighton, Lewes Road, Brighton, BN2 4GJ, United Kingdom

[c]Laboratoire Interdisciplinaire de Physique, Université Grenoble Alpes and CNRS,, F-38000 Grenoble, France

*Corresponding author; e-mail: klaszlo@mail.bme.hu
phone: +36-14631893
fax: +3614633767
postal address: Department of Physical Chemistry and Materials Science, BME, H-1521 Budapest, Hungary

Abstract

Comparison of nitrogen adsorption isotherms of porous carbons before and after exposure to proteins yields information on the pore landscape that is unobtainable from small angle neutron scattering (SANS) [Carbon 2016;106:142–151]. Two globular proteins, bovine serum albumin (BSA), and bovine pancreatic trypsin inhibitor (BPTI), are studied, with two different porous carbon substrates: a hydrophobic open structured carbon aerogel with basic surface pH (C1), and a hydrophilic medical grade microporous carbon with neutral surface pH (C2).

BSA and BPTI both interact more strongly with the hydrophilic carbon than with C1, but C2 adsorbs notably less protein. Both proteins are arrested at the micropore entrances. With increasing concentration in C1, these protein barriers, on drying, seal the micropores hermetically to nitrogen gas. Owing to the adsorbed protein, macropores that are otherwise too wide to be detected in virgin C1 shrink and become detectable by gas adsorption. In C2 the dry protein barriers are looser and remain permeable to nitrogen molecules, leaving the measured micropore and mesopore surface areas practically unaffected. This double probe approach corroborates and extends earlier SANS findings, highlighting the role played by pore structure and the hydrophilic/hydrophobic character of the substrate in protein adsorption.

Keywords: adsorption; protein; BSA; BPTI; carbon aerogel; porosity; surface chemistry

1. Introduction

The immense potential of porous nanostructured carbon materials in biomedical applications remains far from being realised. In biosensor preparations a fundamental step is to immobilise biomolecules, especially proteins, on carbon electrodes, by physicochemical means. [1,2] Nakanishi et al. [3] have drawn attention to the adsorption of proteins on nanocarbons (graphene, nanotubes and fullerenes) as a means of chemically functionalizing the substrate to serve as nanosensor devices. Another significant role is the removal of toxic proteins from body fluids. The effectiveness of these "medical carbons" in haemoperfusion treatment in cases of acute poisoning is well documented. [4] In this procedure toxins are removed from a patient's bloodstream by extracorporeal circulation through activated carbon. [5,6] Porous carbons are also promising candidates for eliminating biologically and chemically resistant pathological proteins, such as prions, from agricultural waste water. These proteins, which survive conventional water treatment processes, invade lakes and rivers. [7]

The solid surface - protein interaction, which is of crucial importance in all these applications, involves different mechanisms including electrostatic, hydrophobic and van der Waals interactions, as well as formation of hydrogen bonds. Even in the case of flat surfaces the resultant effect is a combination of these. The wettability and chemistry (hydrophilic/hydrophobic nature) of solid surfaces have a decisive impact on the molecular interactions.[8,9,10] In porous systems size exclusion and confinement conditions also contribute to this picture.[8] Upon adsorption, proteins can denature or change their conformation, and hence their activity, and thus may present a health hazard. [10,11]

For lysozyme, an enzyme of molecular weight M_W=14.6 kDa, the maximum adsorption on untreated porous carbon surfaces occurs at its isoelectric point, around pH 11. [12] Its high adsorption affinity is attributed to strong hydrophobic interactions between the

non-polar side chains of the amino acid residues and the hydrophobic surface of the carbon. The surface area and the pore volume of ordered mesoporous carbon adsorbent control its adsorption capacity. Oxidative functionalization of the carbon enhances adsorption of the biomolecule through the anchoring capacity of the - COOH groups at the entrance of the mesopores, which can hinder desorption of the protein. [13] Yushin et al. found that the adsorption of cytokines does not result in denaturation of the protein, but that it is determined by the pore size distribution of the activated carbon substrate. [14]

In this study of adsorption on porous carbons, we investigate two globular model proteins, bovine serum albumin (BSA) and bovine pancreatic trypsin inhibitor (BPTI). These were chosen for their widely different mass, size and pH response. BSA is a soft amphiphilic globular protein often used in model studies as a representative of biopollutants. Its loose structure and low isoelectric point (Table 1) make it pH sensitive. At low pH the resulting internal electrostatic repulsion denatures the protein, converting the molecular conformation from globular to an extended chainlike form. [15]

The smaller protein studied, BPTI, also known as aprotinin, is a single polypeptide chain, folded in a stable, compact globular conformation. [16, 17] Its compact structure, high isoelectric point and insensitivity to pH ensure its conformational stability throughout the physiological pH range.

Long et al. [18] have studied the adsorption of BSA from buffer solutions in the pH range 2.35-10 on phenol-melamine-formaldehyde derived carbon aerogels with controlled particle and mesopore size. In this case, as also reported in many other studies, the highest protein uptake was achieved at the isoelectric point of BSA. The authors found that for optimum adsorption capacity the pore size must be slightly larger than the size of the protein. When the pore size is close to that of the protein, the preferred adsorption site is at the pore entrance, thus blocking access to the remainder of the pore that otherwise would be available

for further BSA molecules. If the pore size is appreciably larger than the biomolecule, then the size no longer affects the adsorption capacity. In an investigation of adsorption of BSA and myoglobin (M_w = 17.7 kDa) on porous carbon close to physiological solution conditions (ionic strength 0.15 M, in pH 7.0 buffer) the uptake of the smaller protein was almost more than 3 times greater. The same study proposed that accumulation of the proteins in the macropores is due to both adsorption and self-association.

Adsorption of BSA in carbon nanochannels with controlled surface chemistry from buffered aqueous solutions (pH 7.8. and 9.6) was reported by Vijayaraj et al. [19] Although the adsorption mechanism relies mainly on hydrophobic interactions, uptake correlates with the amount of oxygenated surface groups. (The correlation is stronger if the surface area is small, otherwise mostly hydrophobic interactions prevail.) In spite of carbon samples with wider pores having a smaller surface area, the BSA uptake increases significantly with pore size, a clear demonstration of steric exclusion, with the possible accompaniment of pore blocking.

In the literature, few investigations into protein adsorption on *porous* materials, including carbons, are reported, mainly owing to the limitations of such widely used and powerful methods as quartz crystal microbalance (QCM) or ellipsometry. [20] Observations of adsorption on porous carbon by optical methods, such as FTIR, are tributary to light attenuation, and hence open to the difficulty of discriminating between surface and bulk adsorption. Recently we reported results on the adsorption of BSA and BPTI on porous carbon materials with different pore size distributions and surface chemistry [21] as seen by non-destructive small angle neutron scattering (SANS) and small angle X-ray scattering (SAXS) techniques. [22, 23, 24] These techniques are unique in that they can detect the spatial structure and organisation of molecules adsorbed inside the porous medium. [25]

For a full understanding of how proteins are adsorbed in porous carbons, the use of

both scattering and adsorption approaches is essential. This paper however, shows that the adsorption approach alone using a double probe (in this case, proteins and nitrogen gas) can reveal important additional information that is not accessible to scattering measurements. It focuses on the adsorption of the same proteins in the same two carbons as previously, of different pore size distribution, different surface chemistry and different hydrophobicity. The double probe approach measures not merely the total amount of target molecules adsorbed by the sample, but also how the adsorbed protein modifies the pore landscape of the carbon substrate.

2. Experimental

2.1. Materials

The two porous carbons studied are a resorcinol-formaldehyde based carbon aerogel (C1) possessing an open structure, [22, 24] and a commercial porous carbon made from phenol formaldehyde resin (C2) (MAST Carbon International, UK). [26-28] The two probe proteins, bovine serum albumin BSA (Calbiochem) and BPTI (Sigma-Aldrich) have significantly different molecular weights, radii of gyration and isoelectric points (**Table 1**).

Table 1 Physicochemical characteristics of the model proteins

	BSA	BPTI
Molecular weight, kDa	66.1	6.5
Elemental composition	$C_{2932}H_{4614}N_{780}O_{898}S_{39}$	$C_{284}H_{432}N_{84}O_{79}S_{7}$
Amino acid residues	583	58
Radius of gyration	27.6±0.8 Å [21]	9.8±0.5 Å [21]
Solubility in water	40 g/L [29]	>30 g/L [30]
Isoelectric point	4.8-5.5	10.5

2.2. Methods

2.2.1. Characterization of the carbons

Nitrogen adsorption/desorption isotherms were measured at -196 °C, with a Nova 2000e (Quantachrome, USA) computer controlled volumetric gas adsorption apparatus. The samples were evacuated at 20 °C for 24 hours. The apparent surface area S_{BET} was obtained from the Brunauer – Emmett – Teller (BET) model. [31] The total pore volume V_{tot} was calculated from the amount of nitrogen vapour adsorbed at relative pressure p/p_0 close to 1, on the assumption that the pores are then filled with liquid nitrogen. The pore volume at p/p_0=0.95, $V_{0.95}$, is also evaluated, where the corresponding pore width is 460 Å. The micropore volume (V_μ) was deduced from the Dubinin-Raduskevich (DR) model. [32] The pore size distribution (PSD) was calculated using quenched solid density functional theory (QSDFT) assuming slit shaped pores. [33] Transformation of the primary adsorption data and the (micro)pore analysis were performed by the NOVA2000e ASiQwin 3.0. Water vapour adsorption isotherms of this carbon were measured using a volumetric Hydrosorb apparatus (Quantachrome) at 20 °C, with vapour generated at 100 °C. The pH_{PZC} of these carbons was estimated by the standard pH shift method. [34]

2.2.2. Protein adsorption

The adsorption isotherms of the two proteins were measured by batch method from their aqueous solutions (MilliQ water) at 20 °C, with no added buffer. The contact time of 4 days was determined on the basis of preliminary kinetic experiments. The powdered carbon samples pre-wetted with MilliQ water were equilibrated with protein solutions of various initial concentrations in a thermostated shaker at 20 °C. The final liquid (mL)/carbon (g) ratio was 100:1. Protein concentrations were measured by Ultra Performance Liquid Chromatography (UPLC) (Waters) using a photodiode array (PDA) detector at 280 nm. The adsorbed amount m_a was calculated from $m_a = \frac{(c_0 - c)V}{m}$, where c_0 and c are respectively the

initial and equilibrium concentrations, *V* being the volume of the aqueous protein and *m* is the mass of the carbon sample.

3. Results and discussion

3.1. Characterization of the carbon samples

Figure 1a shows the nitrogen adsorption isotherms of the carbon samples. Although the isotherms of both carbons are of Type IIb, i.e., Type II adsorption isotherm with Type H3 hysteresis [35], their pore structures display significant differences, as revealed by the pore size distributions shown in **Figure 1b**, by the micrographs in **Figure 2** and in the data listed in **Table 2.** C2 is built up of larger spherical units and contains more microporosity than the

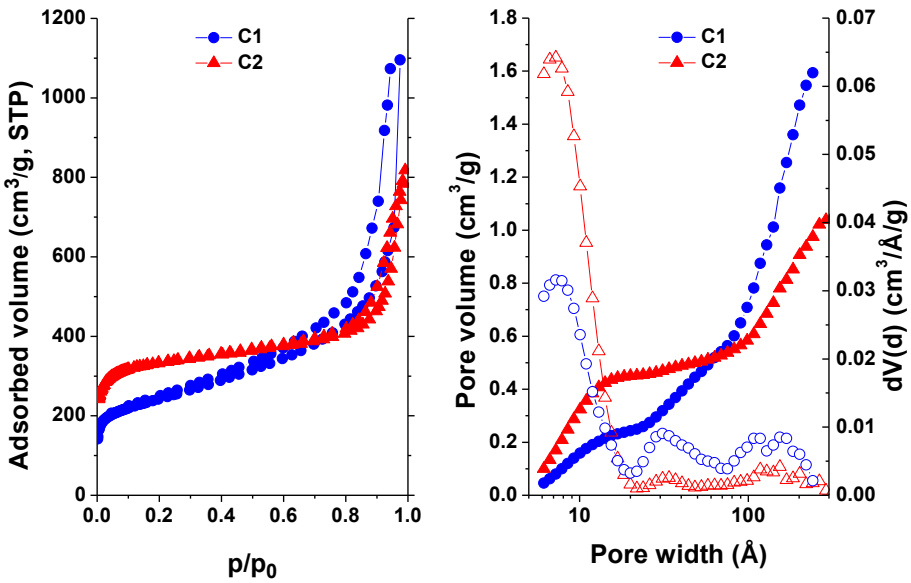

a b

Figure 1. Low temperature nitrogen adsorption isotherms (a) and the cumulative (full symbols) and incremental (open symbols) pore size distributions (PSDs) (b). Circles: C1 carbon, triangles: C2 carbon

looser, mainly mesoporous matrix of C1. While C2 is composed mainly of micropores and wider mesopores (> 100 Å), the incremental distribution of C1 reveals a more even pore size

distribution in the mesopore range. Both samples also contain pores that are wider than the upper detection limit of low temperature nitrogen adsorption.

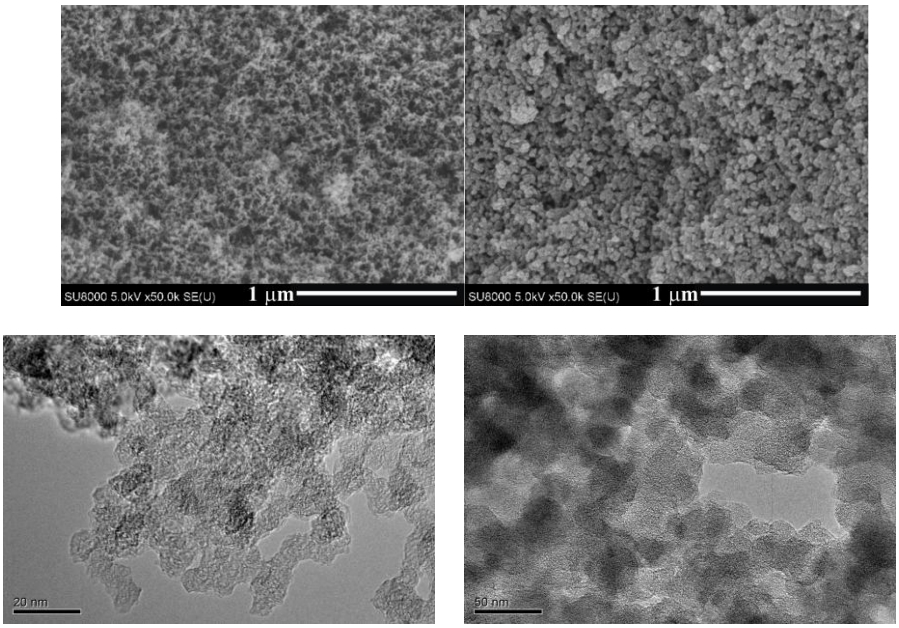

a b

Figure 2. SEM and HRTEM images of the C1 (a) and C2 (b) carbon samples. Scale bars in the HRTEM images are 20 nm and 50 nm for C1 and C2, respectively.

Table 2 Characteristics of carbons measured by nitrogen adsorption (-196 °C)

Sample	S_{BET} m^2/g	V_{tot} cm^3/g	$V_{0.95}$ cm^3/g	V_{μ} cm^3/g
C1	847	1.69	0.80	0.34
C2	1248	1.27	0.96	0.50

* S_{BET}: BET surface area; V_{tot}: total pore volume read at $p/p_0 \rightarrow 1$; $V_{0.95}$: the pore volume at p/p_0=0.95 corresponding to ~460 Å; V_{μ}: micropore volume from DR

The acid/base character of carbon materials is determined by the type and distribution of the functional groups that decorate the surface. The present carbon samples contain only O-containing functional groups, all of which possess a distribution of pK_a values, due to the

effect of the neighboring atoms on the electron cloud [34, 36]. The difference in surface chemistry of the two carbons is reflected in their pH_{PZC}. The pH_{PZC} values are 8.6±0.2 and 6.6±0.3 for carbons C1 and C2 respectively. Below this pH he carbons are positively charged, and above it, negatively charged.

The affinity of the carbons for water was determined from their water vapour adsorption isotherms. The water uptake of C2 is much greater throughout the p/p_0 range. In other words, C2 is more hydrophilic than C1 (**Figure 3**). The water vapour adsorption capacities at the highest p/p_0 values are 0.12 and 0.36 g water/g for C1 and C2, respectively. Comparison of these data with the corresponding values from nitrogen adsorption shows that in C1 the adsorbed water is insufficient to fill the micropores. In C2, by contrast, a significant part of the mesopores is already filled with water at the highest measured relative humidity.

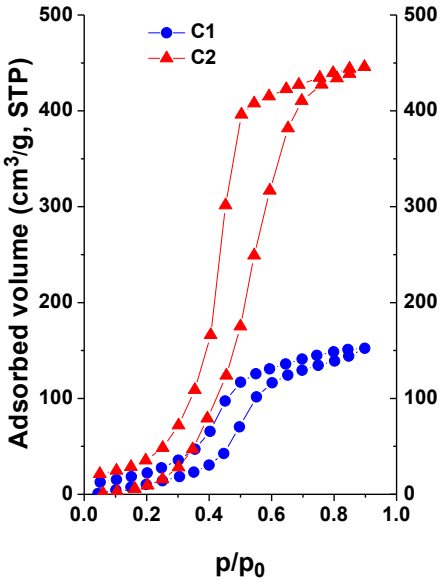

Figure 3. Water vapour adsorption isotherms of the two carbons (20 °C)

3.2. Protein adsorption isotherms

Figure 4 shows the adsorption isotherms of BSA and BPTI from their aqueous solution**.** In order to reproduce the same conditions in the adsorption measurements as were

employed for SANS, no background salt was used in these observations. In contrast to the findings of Ref. [37] the hyperbolic Langmuir model (continuous lines in Figure 4)

$$m_a = \frac{m_m Kc}{1 + Kc} \tag{1}$$

yields an acceptable fit to most of the BSA isotherms, where m_m is the monolayer capacity and K is the equilibrium constant characteristic of the interaction strength. The fitting parameters are listed in **Table S1** of the Supplementary Information**.**

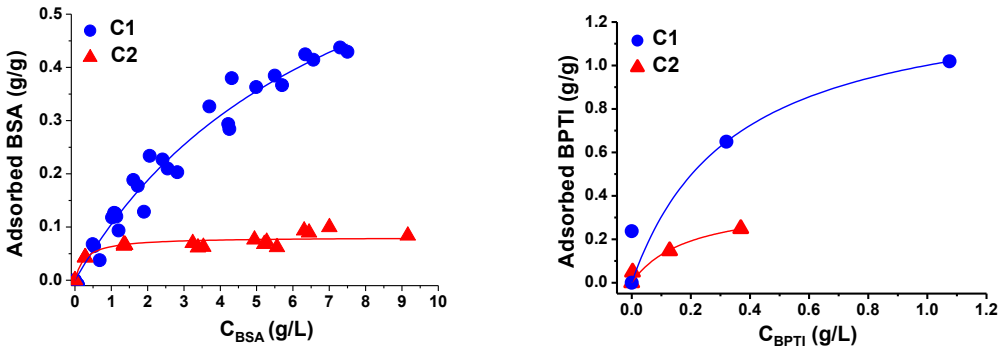

a b

Figure 4: Adsorption isotherms from aqueous protein solutions on C1 and C2 carbons, 20 °C. BSA (a), and BPTI (b) Symbols are measured points, lines are the hyperbolic Langmuir fit.

Desorption measurements in pure water indicate that the BSA uptake is essentially irreversible (less than 3 % of the adsorbed protein is extracted from either carbon). In unbuffered conditions (Figure 4a), the hydrophobic carbon C1 is far from its saturation capacity over the BSA concentration range explored, while the hydrophilic carbon C2 already reaches saturation at c_{BSA}≈1.5 g/L. In spite of its smaller surface area, adsorption by C1 is substantially higher.

For the much smaller protein BPTI (Figure 4b), uptake by both carbons is significantly higher than that of BSA, a clear example of size exclusion. Furthermore, the

interaction of BPTI is stronger than in the BSA-carbon systems. As in Figure 4a, with the hydrophobic carbon C1, the concentration range explored is not sufficiently wide to reach the saturation point.

Under identical conditions, the performance of the two carbons shows that uptake of BSA by the hydrophilic carbon C2 is always lower than in C1, in spite of its higher BET surface area. Furthermore, the larger value found for the parameter K in Eq. 1 indicates that the interaction with C2 is always stronger. These observations demonstrate that that stronger interaction with the substrate entails lower monolayer capacity. For consistency with Ref. [21], in the rest of this paper we use the highest measured adsorption capacity of the isotherms, $m_{a,max}$, instead of the monolayer capacity m_m.

A further comparison between the systems is found by normalising the uptake at the highest measured concentration with respect to the surface area of the carbon. The surface area a_{pr} per protein molecule, expressed in Å^2, is then

$$a_{pr} = \frac{S_{BET}}{\frac{m_{a,\max}}{M_W} \times N_A} \times 10^{20} \qquad (2)$$

where N_{A} is Avogadro's number.

The uptake values listed in **Tables S1-S2** illustrate the effects of size exclusion on large molecules in microporous systems. Although the surface area S_{BET} of C2 is about 50% greater than that of C1, its adsorption capacity for both proteins is smaller than that of C1, thus showing that not all the surface area is accessible for protein adsorption. Also, in both carbons under similar conditions, uptake of the smaller BPTI molecule is significantly larger than that of BSA, as its molecules also have access to narrower adsorption sites within the pores.

3.3. Nitrogen adsorption in the dried BSA loaded samples

Low temperature N_2 adsorption measurements were performed on carbon samples that were dried after being exposed to BSA solutions at ambient pH (**Figure 5**). The effect observed in this case is due to the dried adsorbed protein. The adsorbed BSA gives rise to a systematic depression in the initial part of both sets of the isotherms.

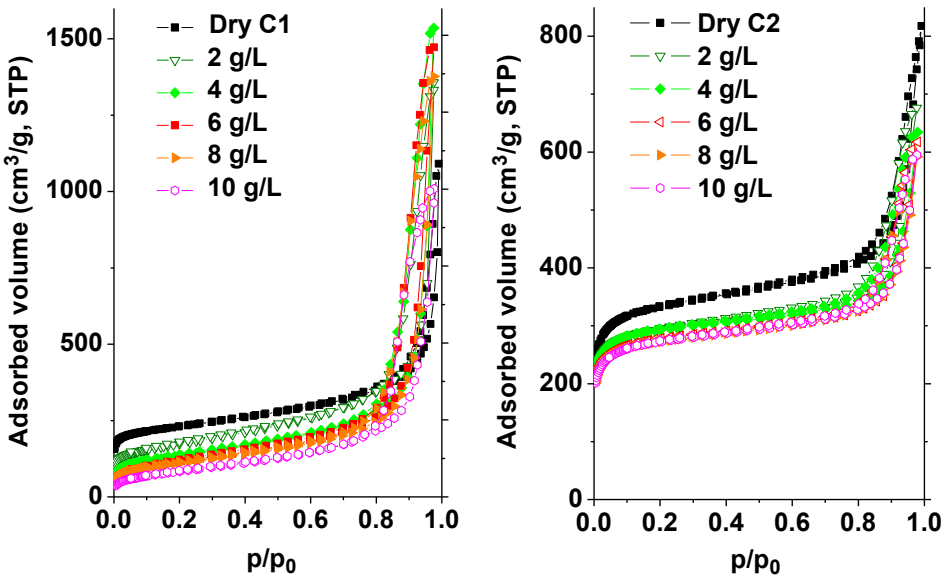

a b

Figure 5. Low temperature nitrogen adsorption/desorption isotherms of BSA loaded carbons C1 (a) and C2 (b)

This depression is accompanied by a gradual decrease in the micropore volume and in the value of S_{BET} derived from the isotherms (**Figure 6**). In the higher relative pressure range of the isotherm, i.e., in the wider mesopore range and beyond, the situation in the two carbons differs. For C2 the total pore volume decreases practically in proportion to the BSA loading, while for C1 it changes in a complex manner (Figure 6c, and Supplementary Material **Table S2**). In the latter case the total pore volume detectable by N_2 increases and displays a maximum some 30 % higher than the pore volume of the virgin C1. This unexpected behaviour can be understood by inspection of the pore size distribution functions. For the

hydrophobic carbon C1 the effect is much more striking over the whole pore size range displayed. The initial part of the incremental distribution extending up to 20 Å shows the influence of the dry adsorbed BSA on the microporous region (**Figure 7**). In C1, nitrogen adsorption decreases strongly with increasing BSA content. This behaviour contrasts with C2, where the adsorption of nitrogen decreases only slightly in the same range. The SANS observations already showed that BSA does not enter the micropores of either carbon [21].

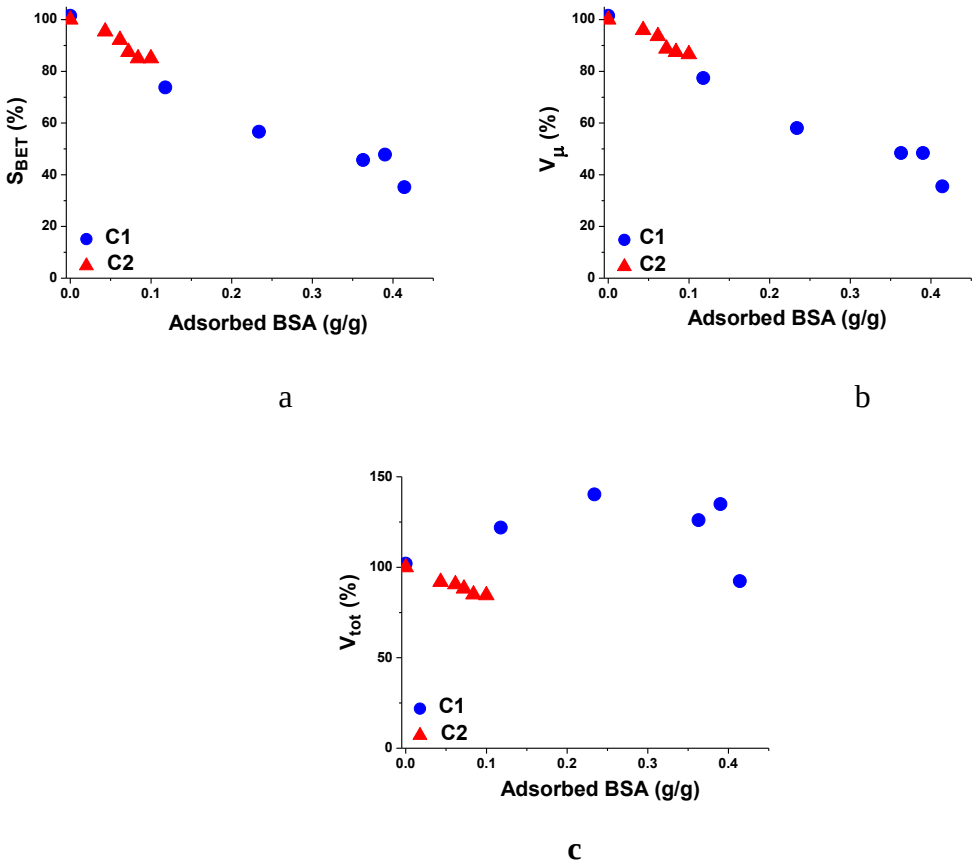

Figure 6. Influence of BSA loading on S_{BET} (a), micropore volume (b) and total pore volume (c)

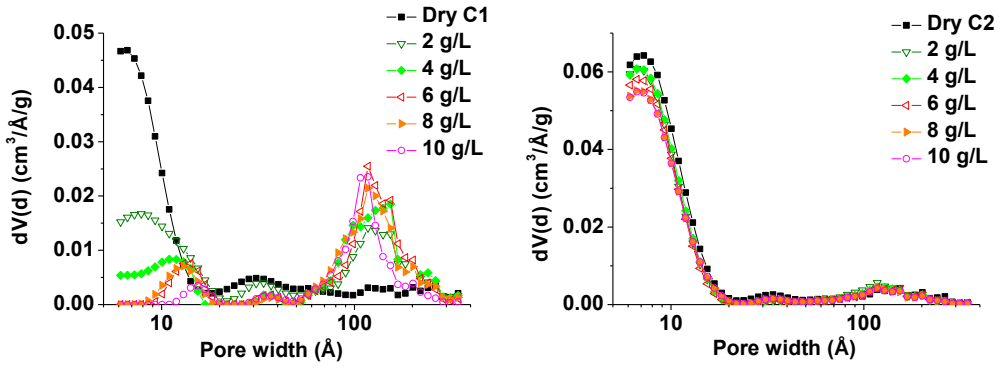

a b

Figure 7. Incremental pore size distributions of BSA loaded C1 (a) and C2 (b) carbons

Around the mouth of the micropores, therefore, the arrangement of the deposited BSA must differt in the two carbons. The SANS measurements showed that in the hydrophobic carbon C1, BSA tends to be adsorbed as a monomer, while in C2 it aggregates into clusters. [21] When the samples are dried, BSA continues to block access of nitrogen to the micropores in C1, but only to a limited extent in C2. Figure 7a demonstrates how pore volume of width less than 50 Å is systematically lost in C1 as protein loading increases, while a new and well defined peak emerges in the 50-200 Å region. This finding indicates that the BSA that accumulates on the walls of the macropores shrinks their effective size into the wider mesopore range, which lies within the measuring window of nitrogen adsorption. In C2, by contrast, wider pores are practically unaffected: here the dry BSA obstructs principally only the entrances to the micropores, but the protein clusters that tend to form in this carbon [21] are loose and porous to nitrogen, and their influence is therefore more limited than in C1 (**Figure 7b**).

3.4. Discussion

The protein adsorption isotherms show that higher uptake corresponds to weaker interaction between the protein and the carbon surface, and *vice versa*. This finding is

counterintuitive, but is consistent with the adsorption measurements on flat surfaces by Jeyachandran et al. [9]. Both proteins establish stronger interaction with the neutral, more hydrophilic, C2 carbon. It implies that the interactions are complex. When immersed in water, the surface of the hydrophobic carbon can be imagined as an electric bilayer, composed on the one hand of the negative π-electrons of the carbon surface and, on the other hand, of the H^+ ions from the water. To achieve this neutral state, the carbon attracts protons from the surrounding water, leaving behind free OH^- groups, thus making the pH of the liquid phase basic. The BSA is slightly above its isoelectric point, and carries a small negative charge, while the hydrophobic carbon C1 is at its $pH_{PZC,}$ in a neutral state. Inside the pores the BSA anions disturb the "electric bilayer" by drawing towards it H^+ ions. This picture, however, is highly simplified and overlooks the distributed nature the electric charges and dipole moments of the BSA molecule. The result nevertheless appears to be that the electrostatic repulsion partially counteracts the attractive hydrophobic interaction between the negative BSA molecules and the carbon surface. The electric charge carried by the BSA generates sufficient electrostatic repulsion towards neighbouring BSA molecules to ensure that they remain mainly as monomers in the adsorbed state.

In the hydrophilic carbon C2 the protein can interact more strongly with the substrate through dipolar interactions and hydrogen bonding, a process that necessarily involves changes in configuration.[9] Both the SANS results [21] and the adsorption measurements of ref. 9 indicate that the electrostatic repulsion between the adsorbed proteins is weakened, thereby favouring the formation of large loose clusters.

For the smaller BPTI molecule below its isoelectric point the overall charge is positive and its interaction with the hydrophilic (i.e., more polar) C2 is stronger, again anchoring the protein and preventing it from entering the narrowest pores. Its interaction with the less polar C1, however, is weaker, which allows the BPTI to diffuse into the mesoporous size range of

pores. Significantly, the SANS results show that, in this case as well, inside the pores of both C1 and C2 the electrostatic repulsion between BPTI molecules is attenuated, leading to the formation of clusters.[21]

It is instructive to compare the two sets of pore size distribution curves with the BSA concentration distribution from the SANS results (**Figure 8**). This representation, in which the greatest contribution to the total concentration comes from the smallest sizes, illustrates the pore size range in which the BSA content of C1 exceeds that in C2. In the hydrophobic carbon C1 a secondary peak in the concentration distribution develops at pore widths $w > 210$ Å, i.e., in the range that still lies within the pore size window detectable by N_2 adsorption. In the neutral carbon C2, the second maximum of the concentration distribution occurs at $w>$ 2000 Å. This pore size range is outside the detection window of gas adsorption. Figure 8 also confirms that the BSA does not penetrate into pores of size smaller than 20 Å. The micropores, which constitute a significant part of the BET surface area, are thus inaccessible to these large molecules.

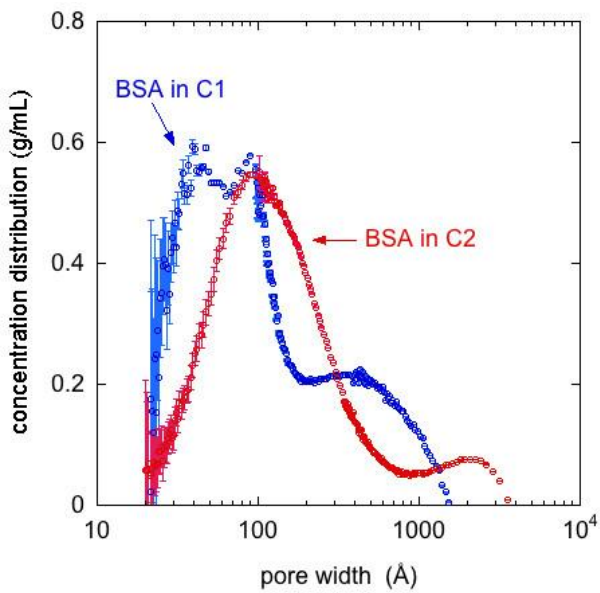

Figure 8. Concentration distribution of BSA in the C1 and C2 carbon particles, plotted as a function of pore width w, defined as $w=2\pi/q$, where q is the neutron scattering momentum transfer. The cut-off at $w\approx 20$ Å ($q \approx 0.31$ Å^{-1}) is the same for both samples. The trend at

w>1000 Å in C1 is an artefact of the measurement (from Ref. 21)

4. Conclusions

This article addresses the question of how proteins are adsorbed on two different porous carbon substrates, a hydrophobic open structured carbon aerogel (C1) with basic surface pH, and a hydrophilic commercial medical grade microporous carbon (C2) suitable for haemoperfusion, having neutral surface pH. The present measurements confirm our earlier observations by small angle neutron scattering, which showed that the proteins are unable to enter the micropores of either carbon.

The protein adsorption measurements described here demonstrate that the interaction between the proteins and C1 is much weaker than that in C2, but that an inverse relationship exists between strength of interaction and amount of protein adsorbed. Gas adsorption measurements performed on the dried protein containing samples reveal the change in the pore landscape imposed by the adsorbed protein. In either carbon both BSA and BPTI settle at, and obstruct, the entrances to the micropores. With rising protein content the micropores in C1 become completely impermeable to nitrogen molecules. Furthermore, as the walls of the wider pores become tiled with the protein, their effective pore size shrinks into the range spanned by gas adsorption measurements. In C2, by contrast, both with BSA and BPTI the protein aggregates are permeable to nitrogen molecules. In this case, the resulting micropore and mesopore surface areas remain practically unaffected by the presence of the proteins.

Two possible applications of porous carbons mentioned in the introduction were, firstly, as a scavenger of toxic proteins: the findings of this paper show that hydrophobic porous carbons offer a promising avenue in the search for tailored carbons. A more speculative application is as a means for storing proteins. In the systems investigated here, however, the rate of protein recovery after adsorption is unacceptably small. Further investigations are required to establish the conditions of electrostatic repulsion that render the

adsorption process reversible.

The present observations provide a glimpse of the information that can be obtained from combined scattering and adsorption measurements. They also show that adsorption measurements alone, using multiple probes, in this case proteins and nitrogen gas, yield independent information about the internal landscape of porous systems that is not otherwise accessible.

Acknowledgements

Financial support from the Marie Curie International Research Staff Exchange Scheme (ENSOR, Grant No. 269267), the Marie Curie Reintegration grant, PERG08-GA-2010-276954, and OTKA K109558 is acknowledged. AT recognizes the support of TÁMOP 4.2.4. A/1-11-1-2012-0001 "National Excellence Program – Elaborating and operating an inland student and researcher personal support system". The project was subsidized by the European Union and co-financed by the European Social Fund.

References

[1] A. Sassolas, L.J. Blum, B.D. Leca-Bouvier, Immobilization strategies to develop enzymatic biosensors, Biotechnology Advances 30 (2012) 489–511.

[2] K. Ariga, K. Minami, L.K. Shrestha, Nanoarchitectonics for carbon-material-based sensors. Analyst 141 (2016) 2629-2638.

[3] W. Nakanishi, K. Minami, L.K. Shrestha, Q. Ji, J.P.Hill, K. Ariga, Bioactive nanocarbon assemblies: Nanoarchitectonics and applications, Nano Today 9 (2014) 378—394.

[4] P.J. Neuvonen, K.T. Olkkola, Oral activated charcoal in the treatment of intoxications. Role of single and repeated doses, Med. Toxicol. Adverse Drug Exp. 3 (1988) 33–58.

[5] S. Sandeman, M. Petersson, S. Wiezell, C. Howell, G. Phillips, Y. Zheng, S. Tennison, S.

Mikhalovsky. Characterising Nanoporous Carbon Adsorbents for Biological Application to Chronic Kidney Disease, Journal of Biomaterials and Tissue Engineering 2 (2012) 40–47.

[6] C.A. Howell, S.R. Sandeman, G.J. Phillips, S.V. Mikhalovsky, S.R. Tennison, A.P. Rawlinson, O.P. Kozynchenko, Nanoporous activated carbon beads and monolithic columns as effective hemoadsorbents for inflammatory cytokines, Int. J. Artif Organs 36. (2013) 624–32.

[7] K. Qin, M. O'Donnell, R.Y. Zhao, Doppel: more rival than double to prion, Neuroscience 141 (1) (2006) 1–8.

[8] J. Meissner, A. Prause, B. Bharti, G.H. Findenegg, Characterization of protein adsorption onto silica nanoparticles: influence of pH and ionic strength, Colloid Polym. Sci. 293 (2015) 3381–3391.

[9] Y.L. Jeyachandran, J.A. Mielczarski, E. Mielczarski, B. Rai, Efficiency of blocking of non-specific interaction of different proteins by BSA adsorbed on hydrophobic and hydrophilic surfaces, J.Colloid Interf. Sci. 341 (2010) 136–142.

[10] O. Moradi, H. Modaress, M. Noroozi, Experimental study of albumin and lysozyme adsorption onto acrylic acid (AA) and 2-hydroxyethyl methacrylate (HEMA) surfaces, J.Colloid Interf. Sci. 271 (2004) 16–19.

[11] S.H.S. Koshari, N.J.Wagner, A.M. Lenhoff, Characterization of lysozyme adsorption in cellulosic chromatographic materials using small-angle neutron scattering, J. Chromatogr. A. 1399 (2015) 45–52.

[12] A. Vinu, M. Miyahara, K. Ariga, Biomaterial immobilization in nanoporous carbon molecular sieves: influence of solution pH, pore volume, and pore diameter. J. Phys. Chem. B 109 (2005) 6436–6441.

[13] A. Vinu, K.Z. Hossian, P. Srinivasu, M. Miyahara, S. Anandan, N. Gokulakrishnan, T. Mori, K. Ariga, V.V. Balasubramanian, Carboxy-mesoporous carbon and its excellent adsorption capability for proteins, J. Mater. Chem. 17 (2007) 1819–1825.

[14] G. Yushin, E.N. Hoffman, M.W. Barsoum, Y. Gogotsi, C.A. Howell, R.R. Sandeman, G.J. Phillips, A.W. Lloyd, S.V. Mikhalovsky, Mesoporous carbide-derived carbon with porosity tuned for efficient adsorption of cytokines, Biomaterials 27 (2006) 5755–5762.

[15] P.J. Sadler, A. Tucker, pH-induced structural transitions of bovine serum albumin histidine pK, values and unfolding of the N-terminus during the N to F transition, Eur. J. Biochem. 212 (1993) 811–817.

[16] P.M. Mannucci, Hemostatic drugs. N. Engl. J. Med. 339 (1998) 245–53.

[17] A.M. Mahdy, N.R. Webster, Perioperative systemic haemostatic agents. British journal of anaesthesia 93 (2004) 842–58.

[18] D. Long, R. Zhang, W. Qiao, L. Zhang, X. Liang, L. Ling, Biomolecular adsorption behavior on spherical carbon aerogels with various mesopore sizes, J.Colloid Interf. Sci. 331 (2009) 40–46.

[19] M. Vijayaraj, R. Gadiou, K. Anselme, C. Ghimbeu, C. Vix-Guterl, H. Orikasa, T. Kyotani, S. Ittisanronnachai, The Influence of Surface Chemistry and Pore Size on the Adsorption of Proteins on Nanostructured Carbon Materials, Adv. Funct. Mater. 20 (2010) 2489–2499.

[20] P. Roach, N.J. Shirtcliffe, D. Farrar, C.C. Perry, Quantification of surface-Bound proteins by fluorometric assay: comparison with quartz crystal microbalance and amido black assay, J. Phys. Chem. B 110 (2006) 20572–20579.

[21] B. Nagy, A. Tóth, I. Savina, S. Mikhalovsky, L. Mikhalovska, I. Grillo, E. Geissler, K. László, SANS study of confinement of globular proteins in porous carbons. Carbon 106 (2016) 142–151.

[22] A.P. Radlinski, M. Mastalerz, A.L. Hinde, M. Hainbuchner, H. Rauch, M. Baron, J.S. Lin, L. Fan, P. Thiyagarajanet, Application of SAXS and SANS in evaluation of porosity, pore size distribution and surface area of coal. International Journal of Coal Geology 59 (2004) 245–271.

[23] K. László, O. Czakkel, B. Demé, E. Geissler, Simultaneous adsorption of toluene and water vapor on a high surface area carbon, Carbon 50 (2012) 4155 – 62.

[24] K. László, O. Czakkel, G. Dobos, P. Lodewyckx, C. Rochas, E. Geissler, Water vapour adsorption in highly porous carbons as seen by small and wide angle X-ray scattering, Carbon 48 (2010) 1038–48.

[25] S.H.S Koshari, N.J. Wagner, A.M. Lenhoff, Characterization of lysozyme adsorption in cellulosic chromatographic materials using small-angle neutron scattering. J. Chromatogr. A. 1399 (2015) 45–52.

[26] R.S. Tennison, Phenolic-resin-derived activated carbons, Applied Catalysis A 173 (1998) 289–311.

[27] V.M. Gun'ko, S.T. Meikle, O.P. Kozynchenko, S.R. Tennison, F. Ehrburger-Dolle, I. Morfin, S.V. Mikhalovsky, Comparative characterization of carbon adsorbents and polymer precursors by small-angle X-ray scattering and nitrogen adsorption methods. J. Phys. Chem. C 115 (2011) 10727–10735.

[28] V.M. Gun'ko, V.V. Turov, O.P. Kozynchenko, V.G. Nikolaev, S.R. Tennison, S.T. Meikle, E.A. Snezhkova, A.S. Sidorenko, F. Ehrburger-Dolle, I. Morfin, D.O. Klymchuk, S.V. Mikhalovsky, Activation and structural and adsorption features of activated carbons with highly developed micro-, meso- and macroporosity, Adsorption 17 (2011) 453–460.

[29] https://www.sigmaaldrich.com/content/dam/sigma-aldrich/docs/Sigma/Product_Information_Sheet/a4919pis.pdf

[30] M. Budayova-Spano, S. Lafont, J.P. Astier, C. Ebel, S. Veesler, Comparison of solubility

and interactions of aprotinin (BPTI) solutions in H_2O and D_2O, Journal of Crystal Growth 217 (2000) 311–319.

[31] S. Brunauer, P. Emmett, E. Teller, Adsorption of gases in multimolecular layers, J. Am. Chem. Soc. 60 (1938) 309–319.

[32] M.M. Dubinin, L.V. Radushkevich, Equation of the characteristic curve of activated. charcoal. Proc. Acad. Sci. USSR Phys. Chem. Sect. 55 (1947) 331–337.

[33] J. Landers, G.Y. Gor, A.V. Neimark, Density functional theory methods for characterization of porous materials, Colloids Surfaces A Physicochem. Eng. Asp. 437 (2013) 3–32.

[34] M. V. Lopez-Ramon, F. Stoeckli, C. Moreno-Castilla, F. Carrasco-Marin, On the characterization of acidic and basic surface sites on carbons by various techniques, Carbon 37 (1999) 1215–21.

[35] F. Rouquerol, J. Rouquerol, K.S.W. Sing, P. Llewellyn, G. Maurin, Adsorption by powders and porous solids. Second edition. Academic Press (2014).

[36] C.A. Leon y Leon, L.R. Radovic, Interfacial chemistry and electrochemistry of carbon surfaces. In: Thrower PA, ed. Ch8emistry and Physics of Carbon, vol. 24, Marcel Dekker; 1994 p. 213-310

[37] A.E. Ivanov, O.P. Kozynchenko, L.I. Mikhalovska, S.R. Tennison, H. Jungvid, V.M. Gun'ko, S.V. Mikhalovsky, Activated carbons and carbon-containing poly(vinyl alcohol) cryogels: characterization, protein adsorption and possibility of myoglobin clearance. Phys. Chem. Chem. Phys. 14 (2012) 16267–16278.

Supplementary material

Table S1

Parameters from the hyperbolic Langmuir fit to protein adsorption isotherms*

Carbon	BSA			BPTI		
	m_m g/g	K L/g	R^2	m_m g/g	K L/g	R^2
C1	0.88	0.13	0.974	1.34	2.92	0.861
C2	0.09	3.30	0.781	0.38	5.26	0.920

* m_m: monolayer capacity, K: equilibrium constant, R^2: coefficient of determination

Table S2 Average surface concentration of the proteins and surface area per protein molecule

Carbon	BSA		BPTI	
	$m_{a,max}$* g/g	a_{pr}** Å^2/molecule	$m_{a,max}$* g/g	a_{pr}** Å^2/molecule
C1	0.42	2.2×10^4	1.03	0.89×10^3
C2	0.09	1.5×10^4	0.27	5.0×10^3

*highest measured adsorption capacity; ** from Eq. (3).